Primary events following electron injection into water and adsorbed water layers

R. N. Barnett and Uzi Landman
School of Physics, Georgia Institute of Technology, Atlanta, Georgia 30332

Abraham Nitzan[a)]
Department of Chemical Physics, Weizmann Institute of Science, Rehovot, 76100, Israel

(Received 25 June 1990; accepted 9 August 1990)

The initial stages of the evolution of an electron injected into bulk water (at 300 K) and into thin water films (1–4 monolayers) adsorbed on a Pt(111) substrate at 50 K are investigated. It is shown that for electrons injected into bulk water with an initial translational kinetic energy between 1.54 and 6.18 eV (i.e., subexcitation energies), the electron momentum time-correlation function $\langle \hat{p}(0)\hat{p}(t)\rangle$, decays to zero on a time scale of less than 1 fs, reflecting strong backscattering of the electron by the water molecules. On this time scale the electron propagation in the medium is dominated by elastic processes. Furthermore, during this initial stage the system is well represented by a static aqueous medium. Transmission of electrons injected into thin films of adsorbed water is also dominated by elastic scattering. The dependence of the electron transmission probability on the film thickness and the initial injection energy are in accord with recent experimental results of photoinjected electrons into adsorbed water films.

I. INTRODUCTION

Injection of an electron into water is an example of a general class of processes in which a fast charged particle penetrates a dense medium.[1] The particular case of an electron and water is of special interest in view of recent experimental[2–5] and theoretical[6–8] advances in the study of the dynamics of electron solvation in water. In such experiments the (excess) electron is formed by photoionization of a water molecule and is ejected into the aqueous medium with an energy of a few eV. The solvated electron is formed after a series of relaxation phenomena on a time scale of a few hundred fs.[2–5] Subsequent time evolution may lead to recapture of the solvated electron by the parent ion[3,4] and the yield of this process depends on the average distance traveled by the electron until it becomes solvated.[3] Thus, it has been argued[3] that the recombination yield is larger in H_2O than in D_2O because of the larger distance travelled in the latter due to smaller efficiency of energy transfer from the fast electron into the softer O–D vibrations.

A similar class of processes involves photoemission at the metal insulator interface, where light absorption induces the emission of fast electrons from the metal into the insulator. Photoemission into water has been studied by several workers.[9,10]

A recent experimental study by Gilton *et al.*[10] demonstrates a new and interesting way to look at transmission of fast electrons through adsorbed water, or xenon, layers. In this experiment several monolayers of water (or xenon) are deposited on Ni (111) at 50 K. A layer of CH_3Cl deposited on top of the insulator layer is used to detect transmitted photoelectrons, which cause fragmentation of this molecule. Monitoring the CH_3 signal as a function of the spacer (water or Xe) thickness and photoelectron energy, yields information about the electron transmission process.

There are several fundamental questions associated with the processes described above:

(a) What is the time scale associated with the initial stage of the electron propagation through the condensed insulator? In the particular experiment of Gilton *et al.*[10] we may ask on what time scale do we expect the electron to go through the water (or Xe) film, given the film thickness and the electron energy?

(b) What is the nature of the electron transport through the disordered condensed medium during the time scale of interest? Is the transport coherent or diffusive in nature?

(c) What is the nature of the collision processes which dominate electron propagation through the medium? Are these primarily elastic or inelastic? What is the time scale for energy transfer between the electron and the medium and what are the solvent modes which are the primary acceptors of the electron energy (i.e., energy dissipation channels)?

(d) How does the electron transport process depend on the nature of the solvent phase (i.e., water vs xenon, and H_2O vs D_2O), on the electron–solvent interaction, and on the initial electron energy?

Of particular interest is the process of energy transfer between the electron and the solvent. In water the process is complete after about 0.5 ps,[2–5] however the electron appears to be localized already after $\sim$0.1 ps.[2–5] Gilton *et al.*[10] have interpreted their observed dependence of the electron transmission signal on the water layer thickness in terms of efficient inelastic scattering and energy loss, lead-

[a)]On leave from Tel Aviv University.

 0021-9606/90/216535-08$03.00

ing to substantial amplitudes of near zero energy states after going through two monolayers of water. Measured total collision cross sections for electron scattering from H_2O molecules in vapor[11] are in the range of $15–20\times 10^{-16}$ cm^2 and the inelastic contribution to this value were estimated to be less than 1×10^{-16} cm^2.[12–15] No data are available for the magnitude of energy loss per inelastic collision but it appears that inelastic scattering cannot account for a total loss of the photoelectron energy after going through two monolayers of water.[16]

Theoretical calculations of the transport of fast electrons through condensed insulating phases usually use stochastic approaches based on multiple isolated collisions (e.g., Boltzmann equations).[17] For lower energy subexcitation electrons (having an energy below the ionization, or electronic excitation, threshold for the medium), the validity of such a description is not clear (even though it was used in several recent works[13–15,18,19]). One way to justify a classical stochastic picture of the electron energy degradation process is to assume that the quantum mechanical phase is efficiently randomized by quasi-elastic interactions. This assumption is implicit in the formalism put forward by Fano and Stephens[20] to describe incoherent energy loss by subexcitation electrons.

In this paper we take a different approach to the problem of electron transmission through water and water films by focusing on the initial stage, i.e., the first few femtoseconds, of the electron's time evolution, following its injection into water. This time evolution is found by direct solution of the time-dependent Schrödinger equation for the electron, with the water molecules treated classically. Our results indicate that: (a) momentum relaxation is very fast, i.e., the electron momentum correlation function nearly vanishes after ~0.5 fs (b) Energy transfer to the water medium is *relatively* slow; practically no energy transfer occurs on a time scale of 1 fs. (c) On the time scale of electron transmission through thin (a few monolayers) water films the water dynamics does not appreciably affect the electron motion, and the main features of the process may be obtained in a model where the electron interacts with a film of static water molecules. In this context, we note that the time span considered in this study is much shorter than the time scales associated with the dynamics of electron solvation in water. As has been discussed elsewhere,[6,7] the dynamics of electron solvation is characterized by (at least) two time scales, the shorter of which, associated with librational motion of the water molecules in the immediate vicinity of the excess electron, occurring in 20–30 fs.

In the next section we describe the system and the method of calculation. In Sec. III results for the electron evolution in bulk water and transmission through thin water films are presented and discussed. We conclude in Sec. IV.

II. MODEL AND METHODS

Our model of bulk water consists of 256 classical water molecules contained in a cubic box (edge length = 37.28 a.u., i.e., a density of 1 g/cm^3) with periodic boundary conditions. For frozen bulk water simulations we have used a system 8 times larger (twice the linear size of the calculational cell). Temperature (300 K for bulk water, 50 K for the water films simulations) is controlled by the stochastic collision method.[21] Intermolecular and intramolecular interactions are given by the RWK2-M model[22] (which includes intramolecular dynamics of the water molecules) and the electron water pseudopotential is that developed by Barnett *et al.*[23] and used extensively in recent studies of excess electron in water and in water clusters.[7,24]

The time evolution of the electronic wave function is obtained using the quantum-classical time-dependent self-consistent field approximation (TDSCF),[25–27] using the split operator FFT technique.[25,28] The velocity Verlet algorithm[21] is used for the dynamical evolution of the classical degrees of freedom, which are coupled to the electron via the expectation value of the electron–molecule interaction potential, evaluated for the instantaneous electronic wave function.

The adsorbed water films were prepared in the following way: First, three layers consisting of 72 Pt atoms per layer were positioned to form the (111) surface of platinum (lattice constant $a = 7.408$ a.u. and nearest-neighbor distance $d_{nn} = 5.238$ a.u.). The initial configuration of the first monolayer of water molecules adsorbed on the static Pt(111) surface is obtained by setting 48 water molecules on the Pt(111) surface in an ordered configuration with the oxygens located above Pt atoms, forming a bilayer homeycomb lattice.[29] This initial structure is chosen in accord with available data on this system.[29] Subsequently, the system is evolved, using the H_2O–Pt potential constructed by Spohr and Heinzinger,[30] at 450 K for 8 ps, cooled to 50 K over a period of 1 ps and equilibrated at 50 K for an additional 2 ps, to allow relaxation of the adlayer structure. Subsequent water layers are formed by first adding 48 water molecules above the previous layer (at 7 a.u. above the average height of the oxygens), followed by repeating the dynamical relaxation procedure described above.

Figure 1 shows a snapshot [viewed from above, and from the side in 1(a) and 1(b), respectively] of the resulting equilibrium structure of one water layer adsorbed on Pt(111) at 50 K. It is seen that the bilayer honeycomb hydrogen-bonded lattice persists though some dislocations can be seen. In addition we note the two characteristic H_2O molecular configurations which occur in this structure; one in which both OH bonds of an H_2O molecule point slightly upward (i.e., forming an angle $\lesssim 90°$ with respect to the surface normal) and thus participating in hydrogen bonding to neighboring molecules, and the other where one of the OH bonds points slightly downwards (participating in hydrogen bonding) and the other OH bond oriented almost along the normal direction.

Figure 2 shows similar snapshots for two adsorbed water layers, demonstrating that at this coverage the ice-like structure of the adsorbate is quite open, i.e., exposing a significant fraction of the underlying metal substrate atoms. At higher coverages the structure of the added water is less ordered (both laterally and orientationally[31]), with

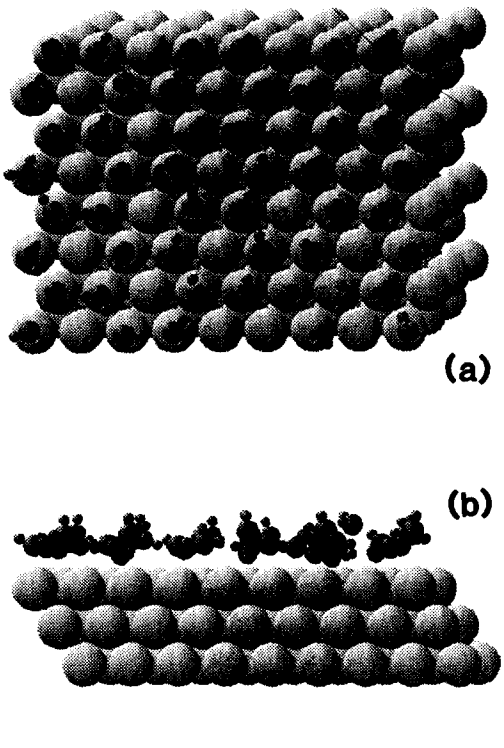

FIG. 1. Snapshot of the equilibrium structure of one layer (48 molecules) of water adsorbed on a Pt(111) surface at 50 K, viewed from above in (a) and from the side in (b). The static Pt substrate consists of three crystalline layers, with 78 atoms/layer (large balls). The oxygens are depicted by the dark medium balls and hydrogens by the smallest balls. Note the almost perfect hexagonal bilayer structure of the adsorbate and the two distinct configurations of the water molecules (see the text).

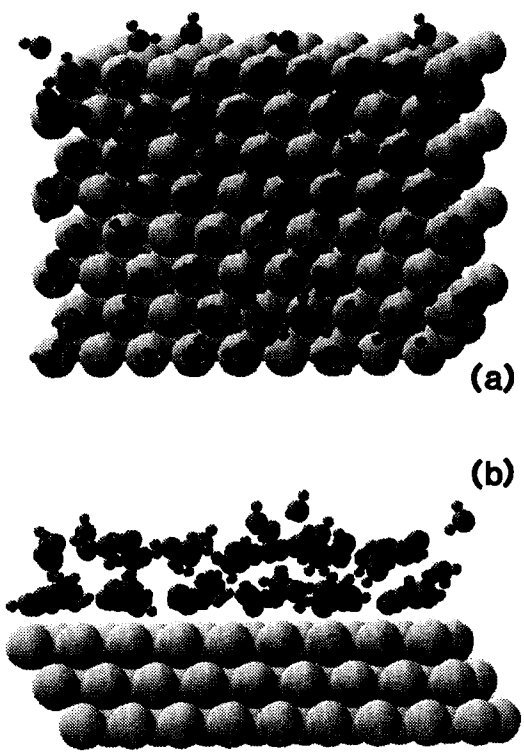

FIG. 2. Same as Fig. 1, for two water layers adsorbed on the Pt(111) substrate at 50 K. Note the ice-like structure, exposing substrate atoms in the middle of the overlayer hexagons.

substrate atoms not exposed, as can be seen from Figs. 3 and 4, corresponding to 3 and 4 water adlayers, respectively. The distributions of distances between the oxygen and hydrogen atoms and the surface metal atoms, for the various water coverages (1–4 layers of water adsorbed on Pt(111) at 50 K), are shown in Fig. 5. Note that in Fig. 5(a) the bilayer structure of the interfacial water is smeared due to fluctuations, while the distinction between OH bond orientations is clear, as seen in Fig. 5(b).

An attempt to solve for the full quantum dynamics of an electron very close to a metal surface involves the complicated issue of the dynamical electron–metal interactions. In the present study we limit ourselves to the role played by the electron–water interaction only. Thus, once the water film was prepared in the manner described above, the metal does not influence the propagation of the electron, and electron transmission and reflection are studied for electrons penetrating the film from the "metal side". While this simulation is not expected to yield quantitative results for comparison with the actual experimental-data,[10] it is adequate for addressing some of the issues raised in Sec. I.

The initial conditions for the quantum simulations are as follows: (i) For simulations of excess electron propagation in bulk water the injected electron is represented initially by a Gaussian wave packet with a specified width and initial momentum, centered about a preexisting cavity, e.g., the location of the center of the ground state distribution of an excess electron, found in a separate calculation for the same (neutral) water configuration. This choice of initial conditions was made, since a random position may result in a very high initial potential energy if the electron wave packet overlaps the core of an oxygen atom. (ii) For the water film simulations the electron is started as a one-dimensional Gaussian, i.e., a Gaussian wave packet in the z (film normal) direction with given initial width and momentum, multiplied by a constant (zero momentum) function of x and y.[32] The center of the Gaussian is located on a surface atom in the topmost layer of the substrate. With reference to this position as the origin ($z=0$), the edge of the first water layer of the adsorbed film (average position of the nearest oxygen plane) is located at $\cong = 4$ a.u. [see, e.g., Figs. 4(b) and 5(a)].

For pure classical dynamics simulations the integration time step used was 2.5×10^{-16} s, while for the mixed quantum-classical evolution the classical time step was 5×10^{-17} s. The quantum evolution of the electron in the bulk water simulations is obtained using a grid of 16^3 points with a grid of spacing 2.33 a.u. In the simulations of electron propagation in frozen bulk water we have used a grid of 32^3 points with the same grid spacing as above. For the water film simulations the grid is $16\times32\times128$ with grid spacings $\Delta x = 2.2681$ a.u., $\Delta y = 1.4732$ a.u. and $\Delta z = 2.0$ a.u. (z is the film normal). The quantum propagation time step was 1.0365×10^{-18} s.

Having described the pertinent details of the simulation method and of the systems' preparation procedures, we turn in the next section to a presentation and discussion of our results.

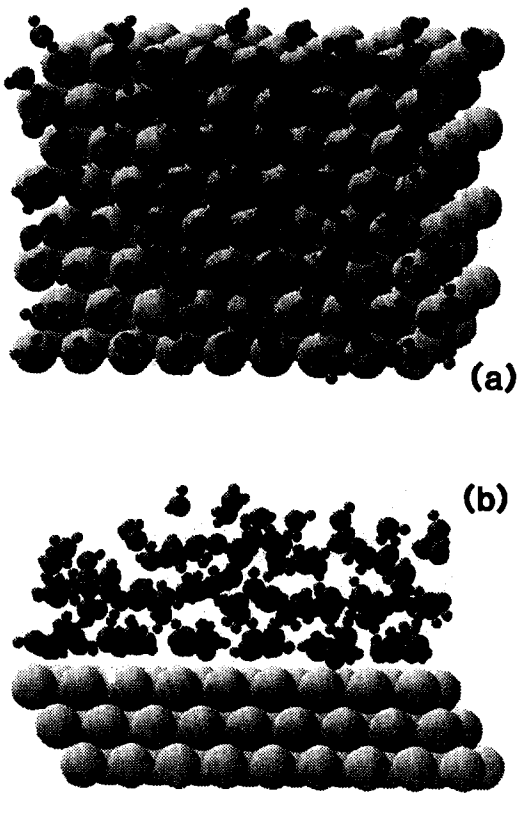

FIG. 3. Same as Fig. 1, for three water layers adsorbed on the Pt(111) substrate at 50 K. Note the more disordered nature of the third layer, and the almost complete lack of exposure of substrate atoms (compare to Fig. 2).

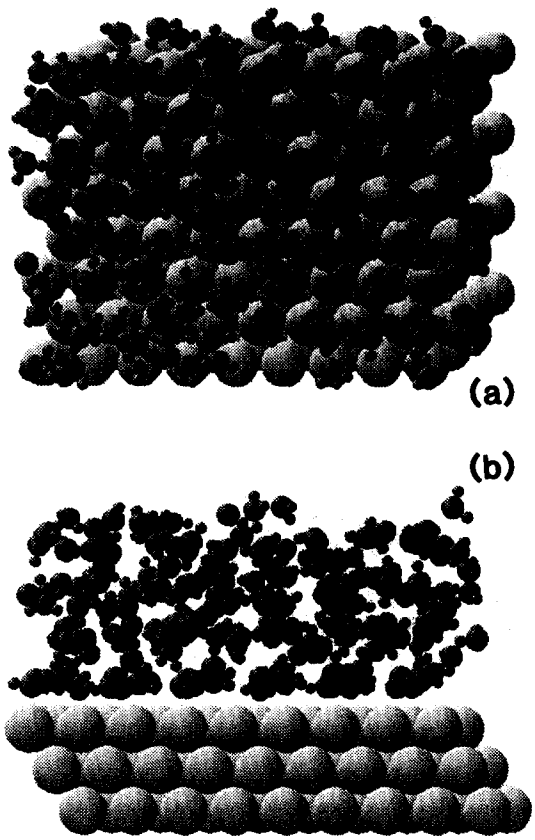

FIG. 4. Same as Fig. 1, for four water layers adsorbed on the Pt(111) substrate at 50 K.

III. RESULTS AND DISCUSSION

A. Bulk water

The first stage of the time evolution of the electron can be characterized by the average position $\langle z \rangle$ of the electron distribution, the average momentum $\langle p_z \rangle$, the overlap of the initial state $\Phi(0)$, with $\Phi(t)$, $C(t) = |\langle \Phi(0) | \Phi(t) \rangle|^2$, and the width of the electron distribution $\sqrt{\langle r^2 \rangle - \langle r \rangle^2}$ [where $\langle\ \rangle$ denotes the expectation value with respect to $\phi(t)$], which are displayed in Figs. 6(a)–6(d). In these figures we compare results obtained using full TDSCF dynamics for both the water and the electron with those obtained by keeping the water configuration static and evolving the electron in this static water configuration, and for two values of the initial momentum, $p_z(0)$, of the wave packet (solid and dashed lines). The starting point in both cases (dynamic and static water) is a randomly chosen configuration for the water, and a Gaussian wave packet of width $\sigma = \sigma_x = \sigma_y = \sigma_z = 1.695$ a.u. for the electron [localization energy $\epsilon_\sigma = 3\hbar^2/(8m\sigma^2) = 3.55$ eV]. This wave packet is centered initially in that preexisting cavity in the water configuration which accommodates it with the lowest potential energy of interaction with the water. The wave packet carries an initial momentum in the z direction. Two values were used: $p_z(0) = 0.674\ 16$ a.u. and $p_z(0) = 0.337\ 08$ a.u. [$p_z(0)^2/2m = 6.18$, and 1.54 eV, respectively].

Figure 6(a) shows the time evolution of $\langle z \rangle$ and $\langle p_z \rangle$, Fig. 6(b) displays the time evolution of $C(t)$, and Fig. 6(c) the time evolution of the widths. The most important observation here is that for the time scale shown, differences in the above quantities, characteristic to the electron, obtained for either propagation in static or dynamic aqueous media are nonresolvable; i.e., the evolution of the electron is not affected by the dynamics of the water molecules, in the femtosecond time scale. This point is emphasized in Fig. 6(d), where we plot against time (for both values of initial momentum) the overlap $|\langle \Phi_s(t) | \Phi_d(t) \rangle|^2$ between the electronic wave function (Φ_d) obtained with the full water dynamics, and that (Φ_s) corresponding to electron propagation in the static water structure. As seen the overlap remains close to unity throughout the 1.3 fs evolution, for both values of initial momentum. The near invariance of the results, obtained via the two procedures, provides an *a posteriority* justification for the use of the TDSCF approximation in the dynamic calculation.

This observation also implies that on the time scale discussed, energy transfer from the electron to the water is negligible. This is indeed seen in Fig. 7, where the electron energy as a function of time is shown [for $p_z(0) = 0.674\ 16$ a.u.]. It should be noted that these results are valid only for

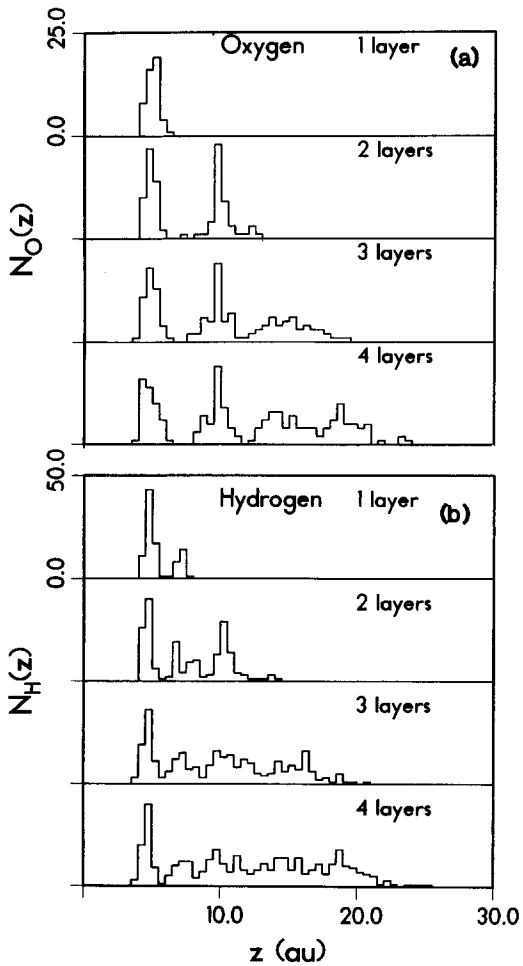

FIG. 5. Number distributions vs distance from the surface (z) of the oxygens (a) and hydrogens (b) of water molecules adsorbed on a Pt(111) substrate at 50 K, for four different coverages (1 layer = 48 H_2O molecules). The origin is taken at the center of the Pt atoms in the topmost layer of the crystalline substrate. Note the bimodal distribution of the molecular hydrogens (in b, most clearly seen for 1 and 2 layers) reflecting the distinct molecular configurations mentioned in the text.

initial electron energies lower than the threshold[33] ($\sim$7.4 eV) for electronic excitation of the water molecule. In view of the large mass disparity between the electron and the atomic constituents of H_2O we do not anticipate that our conclusions be modified by quantum treatment of the solvent.

Further information about the short time evolution of an electron wave packet in bulk water is given in Figs. 8(a)–8(c) which were obtained in a frozen water simulation. In Fig. 8(a) the average position $\langle z\rangle$ as a function of time is shown for a Gaussian wave packet starting with $\sigma_x=\sigma_y=\sigma_z=1.695$ a.u. and an initial $p_z(0)=0.5056$ a.u. (corresponding to a total kinetic energy 7.52 eV divided about equally between localization and translational energy). Also shown is $\langle z\rangle_0$, the position of the same wave packet evolving in free space. In Fig. 8(b) we show similar results for the width of the wave function, $\sigma_z(t)$ and σ_{z0}, showing that on the time scale considered, this quantity increases in the water almost as fast as for the free particle;

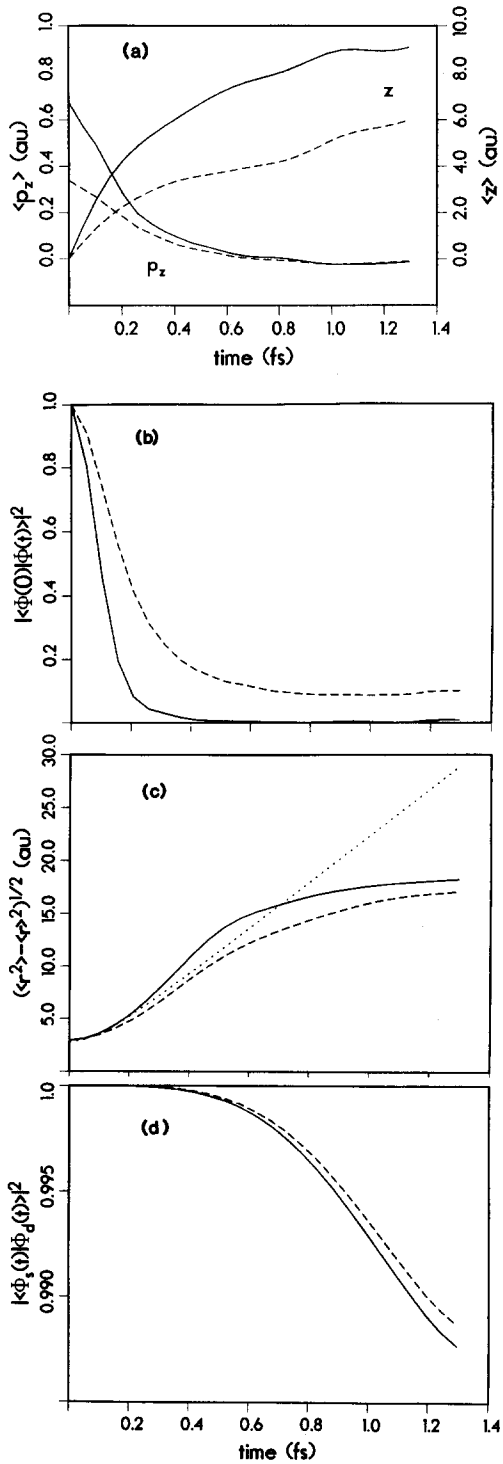

FIG. 6. Short-time (1.3 fs) evolution of an electron in bulk water. Results are given for two initial momenta of the Gaussian wave packet representing the electron [$p_z(0)=0.674\,16$ a.u. (solid lines) and 0.337 08 a.u. (dashed lines)] corresponding to translational energies of 6.18 and 1.54 eV, respectively. (a) Expectation value of the momentum in the propagation direction ($\langle p_z\rangle$, left axis), and the position expectation value ($\langle z\rangle$, on the right axis), vs time. (b) Magnitude squared of the overlap of the initial wave function $\Phi(0)$ with that at time t, $\Phi(t)$, vs time. (c) Width of the wave functions vs time. The width of the wave packet propagating in free space is shown for comparison (dotted line). (d) Magnitude squared of the overlap of the electronic wave functions vs time for electron propagation in static (Φ_s) and dynamic (Φ_d) bulk water. The results in (a), (b), and (c) are for electron propagation in static and dynamic (i.e., full TDSCF) water, which are indistinguishable. All quantities are in atomic units (a.u.) and time in fs.

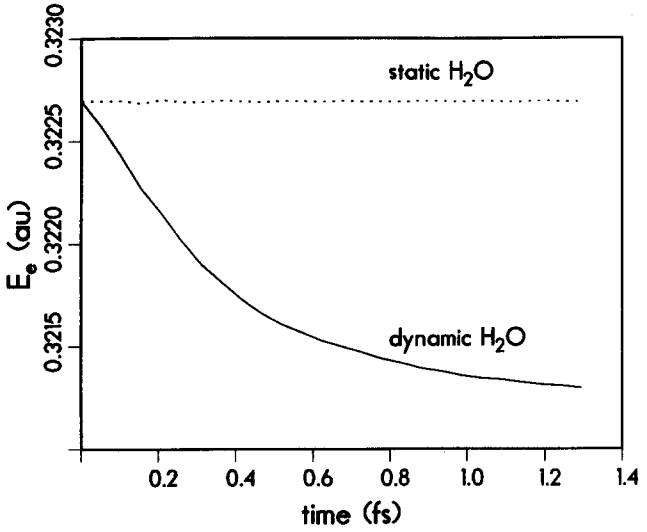

FIG. 7. The electronic energy E_e for an electron with an initial momentum $p_z(0) = 0.674\,16$ a.u. (i.e., translational energy of 6.18 eV), propagating in static (dashed) and dynamic (solid) bulk water vs time. Note the very small change in the electronic energy (for propagation in the dynamic aqueous medium) over the 1.3 fs time span.

significant departure of the two quantities occurs only for $t > 1$ fs. Also displayed is σ_x for the electron propagating in water, showing that the spread of the wave function normal to the propagation direction is somewhat smaller than σ_z. This difference between σ_x and σ_z develops before the average momentum relaxes, for $t < 0.5$ fs [see Fig. 7(c)].

Another view of the momentum relaxation of an injected electron into bulk water is seen in Fig. 8(c) which displays the decay of the momentum time-correlation function $C_p(t) = \langle \Phi(t=0) | \hat{p}\ (0)\hat{p}(t) | \Phi\ (t=0) \rangle$ [divided by $\langle \hat{p}(0)^2 \rangle$] where $\hat{p}(t) \equiv e^{iHt}\hat{p}e^{-iHt}$. For the chosen initial state the characteristic decay time is of the order of 0.5 fs, indicating strong scattering of the electron by the water molecules. This characteristic time depends on the initial state.

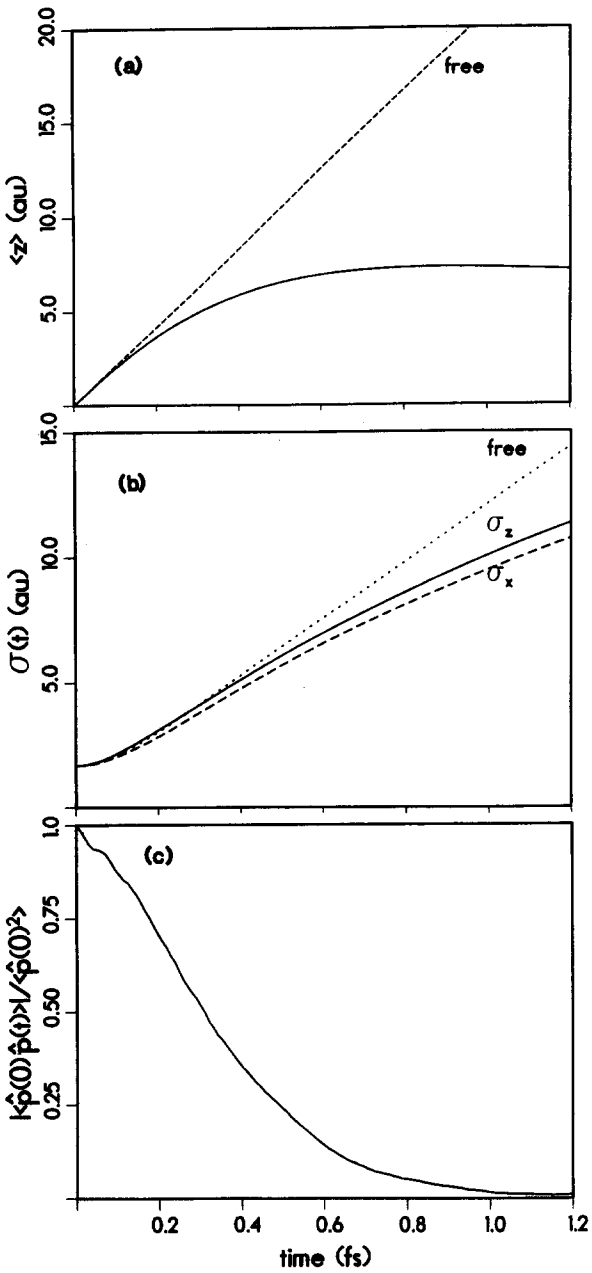

FIG. 8. Electron propagation in bulk water, with an initial momentum $p_z(0) = 0.5056$ a.u. (solid lines). Also shown (dashed lines) are the corresponding quantities for propagation of a free electron with the same initial width and momentum. Shown versus time are: (a) the position expectation value $\langle z \rangle$; (b) the width of the electronic wave function $\sigma(t)$, decomposed into components along (σ_z) and normal (σ_x) to the direction of the initial momentum; (c) the momentum time-correlation function $\langle \hat{p}(0)\hat{p}(t) \rangle / \langle \hat{p}(0)^2 \rangle$. All quantities are given in a.u., and time in fs.

B. Water film

Figure 9(a) displays the integrated outgoing electron current in the z direction, at $z = 28$ a.u., as a function of time, starting from a one-dimensional Gaussian wave packet ($\sigma_z = 2.5465$ a.u., corresponding to a kinetic energy of localization of 0.52 eV) centered initially at $z = 0$ (i.e., at the topmost "metal plane"). The initial momentum of the injected electron is $p_z(0) = 0.589\,05$ a.u. (corresponding to a translational kinetic energy of 4.72 eV). Shown are results for films of 1 to 4 layers of water molecules. Similar results for the reflected integrated current at $z = -6$ a.u. are shown in Fig. 9(b) (Note that at $t \to \infty$, for the present frozen water simulation, the two integrated currents should sum up to 1). Results obtained starting with a three-dimensional Gaussian wave packet ($\sigma_x = \sigma_y = \sigma_z = 2.5465$ a.u.; $p_x = p_y = 0$ and $p_z = 0.589\,05$ a.u.) are only weakly dependent on the starting point in the x,y plane and are almost identical to those obtained using the one-dimensional initial Gaussian. However, both the transmission and reflection probabilities depend strongly on the initial translational energy as is seen in Fig. 9(c). Here the time evolution of the integrated outgoing electron current at $z = 28$ a.u. is shown for two film thicknesses, corresponding to 1 and 3 layers of adsorbed water and for two different initial conditions: $p_z(0) = 0.58905$ a.u. and $p_z(0)$

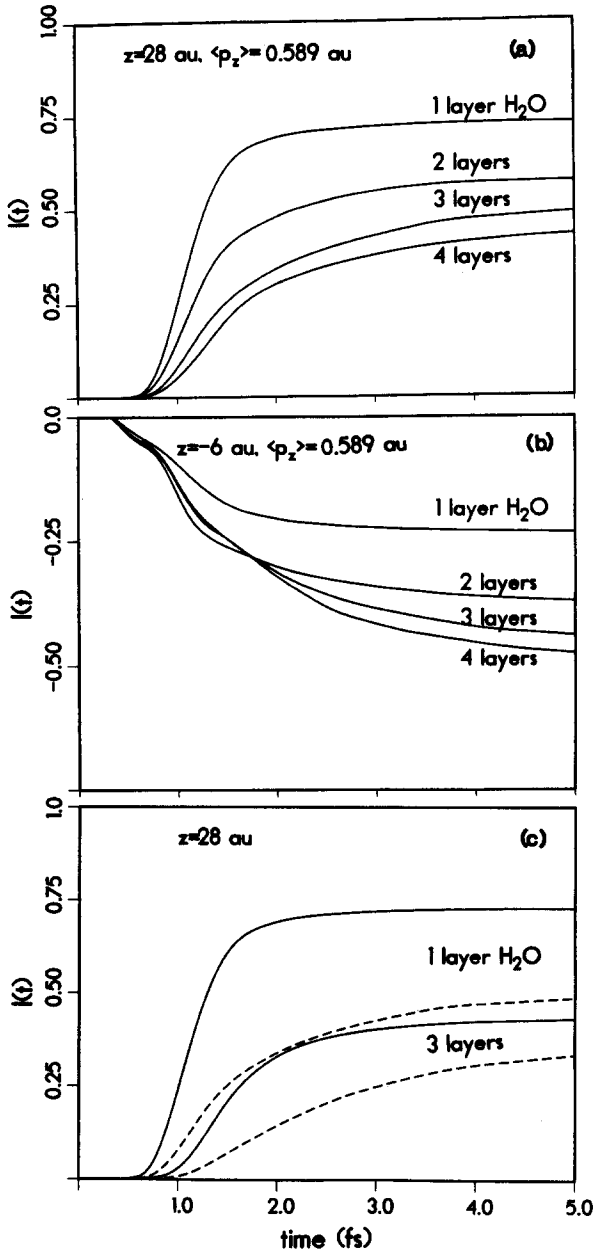

FIG. 9. Electron propagation through adsorbed water films. Integrated current $I(t)$ vs time for an electron represented by a one-dimensional Gaussian wave packet centered initially at $z = 0$, i.e., on the topmost metal plane [with initial momentum $p_z(0) = 0.589$ a.u. and width $\sigma_z = 2.5465$ a.u., corresponding to an initial translational kinetic energy of 4.72 eV and localization energy of 0.52 eV]. (a) $I(t)$ for different thicknesses of the adsorbed water films, at $z = 28$ a.u. (b) $I(t)$ at $z = -6$ a.u. (i.e., reflected current). (c) $I(t)$, at $z = 28$ a.u. for electron propagation through adsorbed films corresponding to 1 and 3 water layers, for two values of the initial momentum, $p_z(0) = 0.589$ a.u. (solid lines) and 0.295 a.u. (dashed lines), corresponding to initial translational kinetic energy of 4.72 and 1.2 eV, respectively. Time in fs.

$= 0.294\,53$ a.u. (translational kinetic energies 4.72 and 1.2 eV, respectively). σ_z is, as before, 2.5465 a.u.

Finally, in Fig. 10, we summarize the thickness dependence of the asymptotic (taken at $t = 5$ fs) electron transmission probability for the two injection energies. Both the thickness dependence and the initial energy dependence are

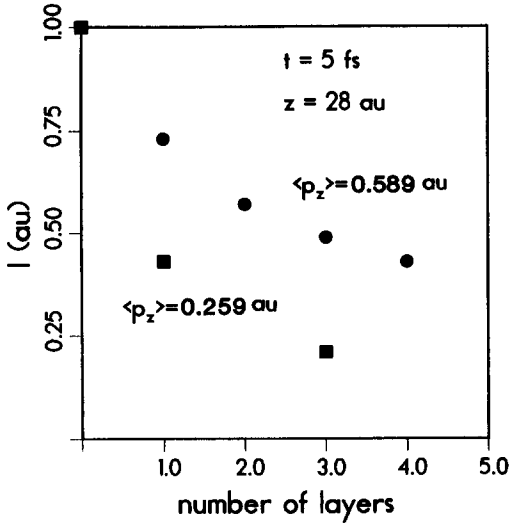

FIG. 10. Summary of the integrated transmitted electron current $I(t)$, vs the number of adsorbed water layers, for $t = 5$ fs at $z = 28$ a.u. Results are shown for two initial momenta of the injected electron, $p_z(0) = 0.589$ a.u. (circles) and $p_z(0) = 0.259$ a.u. (squares).

in good qualitative agreement with the observations made by Gilton *et al.*[10,34] It is seen that on such time scales and for such film thickness, elastic electron scattering from essentially static water molecules can account for the gross features of the total transmission probability.

IV. SUMMARY AND CONCLUSIONS

The penetration of a subexcitation electron into water is followed by a succession of relaxation phenomena which eventually lead to the formation of the fully solvated electron. The final stages of this process are being unravelled by current experimental and theoretical work.[2–8] In the present paper we have focused on the very initial stage of this process exploring time scales of the order of 1 fs where the electron propagation is well represented by the corresponding process in a frozen water environment. This time scale is relevant for the (essentially elastic) scattering of an electron from, and its transmission through, adsorbed water layers. On this time scale the electron momentum correlation function practically relaxes to zero, the characteristic relaxation time is $\lesssim 0.5$ fs, indicating strong backscattering of the electron by the water molecule.

Our studies of the transmission of injected electrons through films of water molecules created to mimic the structure of deposited water layers on Pt(111) at 50 K, indicate that the transmission of subexcitation electrons through such thin (1–4 layers) water films is dominated by elastic scattering. The thickness and energy dependence of the transmission probability which we calculated are in qualitative agreement with recent experimental results.[10] We conclude that the dynamics of the water molecules is not an essential ingredient in determining total transmission probabilities under the specified conditions. Obviously other experimental observables (such as energy resolved transmission probabilities of electrons injected into

adsorbed water films) would enable investigations of inelastic processes, and thus probe the molecular dynamics of adsorbed water layers.

ACKNOWLEDGMENTS

We thank J. P. Cowin for a stimulating discussion. This research was supported by the U. S. Department of Energy Grant No. FG05-86ER45234, the Israel Academy of Science, and by the Israel–U.S.A. Binational Science Foundation.

[1] See, e.g., S. Lencinas, J. Burgdorfer, J. Kemmler, O. Heil, K. Kroneberger, N. Keller, H. Rothand, and K. O. Groenveld, Phys. Rev. A **41**, 1435 (1990), and Refs. 1–10 therein.
[2] A. Migus, Y. Gaudel, J. L. Martin, and A. Antonetti, Phys. Rev. Lett. **58**, 1559 (1987).
[3] A. C. Chernovitz and C. D. Jonah, J. Phys. Chem. **92**, 5946 (1988).
[4] H. Lu, F. H. Long, R. M. Bowman, and K. B. Eisenthal, J. Phys. Chem. **93**, 27 (1989); F. H. Long, H. Lu, and K. B. Eisenthal, Chem. Phys. Lett. **160**, 464 (1989).
[5] F. H. Long, H. Lu, and K. B. Eisenthal, Phys. Rev. Lett. **64**, 1469 (1990).
[6] R. J. Rossky and J. Schnitker, J. Phys. Chem. **92**, 4277 (1988).
[7] (a) R. N. Barnett, U. Landman, and A. Nitzan, J. Chem. Phys. **89**, 2248 (1988); (b) **91**, 5567 (1989); (c) R. N. Barnett, U. Landman, G. Rajagopal, and A. Nitzan, Isr. J. Chem. **30**, 85 (1990).
[8] J. S. Bader and D. Chandler, Chem. Phys. Lett. **157**, 501 (1989).
[9] T. E. Furtak and K. L. Kliewer, Comments Solid State Phys. **10**, 103 (1982).
[10] T. L. Gilton, C. P. Dehnbostal, and J. P. Cowin, J. Chem. Phys. **91**, 1937 (1989).
[11] L. Brescansin, M. A. P. Lima, T. Gibson, V. McKoy, and W. M. Huo, J. Chem. Phys. **85**, 1854 (1986).
[12] C. Szmythowski, Chem. Phys. Lett. **136**, 363 (1987).
[13] M. Michaud and L. Sanche, Phys. Rev. A **36**, 4684 (1987).
[14] M. Michaud and L. Sanche, Phys. Rev. A **36**, 4672 (1987).
[15] M. Michaud and L. Sanche, Phys. Rev. A **30**, 6067 (1984); The inelastic scattering cross section is directly measured in Ref. 14. The analysis of the data using the theory in this paper (Ref. 15) seems to underestimate the elastic cross section.
[16] Using the bare work function of Ni ($\sim$5.1 eV), the initial energy of an electron photoemitted by an incident light at 248 nm (used in Ref. 10) will be near zero. Obviously the metal work function will be considerably lowered in the presence of water adlayers, resulting in an increase of the initial energy of the photoemitted electron.
[17] S. Lencinas, J. Brugdorfer, J. Kemmler, O. Heil, K. Kronenberger, N. Keller, H. Rothard, and K. O. Goeneveld, Phys. Rev. A **41**, 1435 (1990), and references therein.
[18] T. Goulet, J.-P. Jay-Gerin, and J. Patau, J. Electron. Spectrosc. Relat. Phenom. **43**, 17 (1987).
[19] T. Goulet and J.-P. Jay-Gerin, J. Phys. Chem. **92**, 6871 (1988).
[20] U. Fano and J. A. Stephens, Phys. Rev. B **34**, 438 (1986).
[21] J. R. Fox and H. C. Anderson, J. Phys. Chem. **88**, 4019 (1984).
[22] J. R. Reimers and R. O. Watts, Chem. Phys. **85**, 83 (1984).
[23] R. N. Barnett, U. Landman, C. L. Cleveland, and J. Jortner, J. Chem. Phys. **88**, 4421 (1988).
[24] R. N. Barnett, U. Landman, C. L. Cleveland, and J. Jortner, J. Chem. Phys. **88**, 4429 (1988); R. N. Barnett, U. Landman, S. Dhar, N. R. Kestner, J. Jortner, and A. Nitzan, *ibid.* **91**, 7797 (1988); see also Ref. 7.
[25] R. Kosloff, J. Phys. Chem. **92**, 2087 (1988), and references therein.
[26] See Ref. 7.
[27] R. Alimi and R. B. Gerber, Phys. Rev. Lett. **64**, 1453 (1990), and references therein.
[28] M. D. Feit, J. A. Fleck, and A. Steiger, J. Comput. Phys. **47**, 412 (1982).
[29] P. A. Thiel and T. E. Madey, Surf. Sci. Rep. **7**, 211 (1987), and references therein.
[30] E. Spohr and K. Heinzinger, Ber. Bunsenges. Phys. Chem. **92**, 1358 (1988).
[31] K. Foster, K. Raghavan, and M. Berkowitz, Chem. Phys. Lett. (to be published).
[32] Using a three-dimensional Gaussian instead of the one-dimensional Gaussian wave packet yielded almost identical results for one water monolayer. Employing a one-dimensional Gaussian, as described in the text, has the advantage of affecting an average over the initial injection locations in the plane parallel to the adsorbed water film.
[33] R. L. Platzman, Radiation Res. **1**, 2 (1955).
[34] Note that in the experiments described in Ref. 10 the CH_3 signal, which monitors the integrated electron current at the outer edge of the water layer, goes down for water coverage smaller than 2 monolayers. This phenomenon is probably associated with back transfer of the electron to the metal before fragmentation of the methyl chloride takes place, and cannot of course be reproduced by our simulations.